Journal of Steroid Biochemistry and Molecular Biology 243 (2024) 106561

Contents lists available at ScienceDirect

Journal of Steroid Biochemistry and Molecular Biology

journal homepage: www.elsevier.com/locate/jsbmb

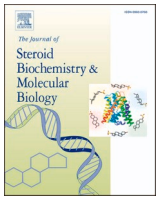

Mitochondrial dysfunction results in enhanced adrenal androgen production in H295R cells

Déborah Mathis [c,1], Therina du Toit [b,d,1], Emre Murat Altinkilic [a,b], Darko Stojkov [e], Christian Urzì [c,f,g], Clarissa D. Voegel [d], Vincen Wu [h], Nicola Zamboni [h,i], Hans-Uwe Simon [e,j], Jean-Marc Nuoffer [a,b,c], Christa E. Flück [a,b], Andrea Felser [a,b,*,2]

[a] Division of Pediatric Endocrinology, Diabetology and Metabolism, Department of Pediatrics, Bern University Hospital, University of Bern, Switzerland
[b] Department for BioMedical Research, Bern University Hospital, University of Bern, Switzerland
[c] University Institute of Clinical Chemistry, Inselspital, Bern University Hospital, University of Bern, Switzerland
[d] Department of Nephrology and Hypertension, Bern University Hospital, University of Bern, Switzerland
[e] Institute of Pharmacology, University of Bern, Switzerland
[f] Magnetic Resonance Methodology, Institute of Diagnostic and Interventional Neuroradiology, University of Bern, Switzerland
[g] Graduate School for Cellular and Biomedical Sciences, University of Bern, Bern, Switzerland
[h] Institute of Molecular Systems Biology, ETH Zurich, Switzerland
[i] PHRT Swiss Multi Omics Center, Zurich, Switzerland
[j] Institute of Biochemistry, Brandenburg Medical School, Neuruppin, Germany

ARTICLE INFO

Keywords:
Mitochondrial dysfunction
Androgen
DHEA
Rotenone
Citrate

ABSTRACT

The role of mitochondria in steroidogenesis is well established. However, the specific effects of mitochondrial dysfunction on androgen synthesis are not fully understood. In this study, we investigate the effects of various mitochondrial and metabolic inhibitors in H295R adrenal cells and perform a comprehensive analysis of steroid and metabolite profiling. We report that mitochondrial complex I inhibition by rotenone shifts cells toward anaerobic metabolism with a concomitant hyperandrogenic phenotype characterized by rapid stimulation of dehydroepiandrosterone (DHEA, 2 h) and slower accumulation of androstenedione and testosterone (24 h). Screening of metabolic inhibitors confirmed DHEA stimulation, which included mitochondrial complex III and mitochondrial pyruvate carrier inhibition. Metabolomic studies revealed truncated tricarboxylic acid cycle with an inverse correlation between citric acid and DHEA production as a common metabolic marker of hyperandrogenic inhibitors. The current study sheds light on a direct interplay between energy metabolism and androgen biosynthesis that could be further explored to identify novel molecular targets for efficient treatment of androgen excess disorders.

1. Introduction

Androgens are steroid hormones essential for reproduction and sexual development that are produced in the human fetal adrenals, adult adrenal zona reticularis (ZR), and gonads of both males and females [1]. Steroidogenesis in the ZR requires a catalytic cascade of specific enzymes and cofactors that are located in the mitochondria and endoplasmic reticulum (ER). Mitochondria play an indispensable role in the initiation of steroid synthesis, as they contain the cholesterol side-chain cleavage enzyme (CYP11A1) on the inner mitochondrial membrane, which represents the enzymatic rate-limiting step in the cellular capacity for pregnenolone synthesis [2,3]. The further conversion of pregnenolone to androgens requires two essential enzymes, namely cytochrome P450c17 (CYP17A1) and 3β-hydroxysteroid dehydrogenase type 2 (HSD3B2). CYP17A1 is a NADPH-dependent enzyme localized on the ER membranes that can catalyze 17α-hydroxylase and 17,20-lyase biosynthetic activities. HSD3B2 is a NAD+-dependent dehydrogenase with distinct subcellular localizations in the ER or mitochondria [3,4].

* Correspondence to: Division of Pediatric Endocrinology, Diabetology and Metabolism, Department of Pediatrics, Inselspital University Hospital, Bern, Switzerland.
E-mail address: andrea.felser@insel.ch (A. Felser).
[1] Contributed equally
[2] ORCID-ID 0000–0003-4806–2940

https://doi.org/10.1016/j.jsbmb.2024.106561
Received 15 March 2024; Received in revised form 20 May 2024; Accepted 6 June 2024
Available online 10 June 2024

Reprogramming of the steroidogenic pathway in the ZR towards dehydroepiandrosterone (DHEA) synthesis is characterized by low expression of HSD3B2 and increased 17,20-lyase activity through increased expression of the allosteric activator cytochrome b5A (CYB5A) [5]. Thus, androgen synthesis depends on a complex intraorganellar interplay between the mitochondrial and ER compartments.

Premature adrenarche (PA) and polycystic ovary syndrome (PCOS) are two common hyperandrogenic conditions in females [6,7]. Adrenarche represents the postnatal development of the ZR in prepubertal children. PA is characterized by early maturation of the ZR and concomitant development of secondary sexual characteristics, typically before 8 years of age in girls, which may progress to PCOS [8,9]. PCOS is a multisystem disorder with reproductive and metabolic perturbations characterized by hyperandrogenism with oligo- or anovulation and polycystic ovaries, and is often associated with insulin resistance, dyslipidemia and obesity. Recent studies have described mitochondrial gene mutations in patients with PCOS, suggesting that mitochondrial dysfunction may be involved in the development and progression of PCOS [10–13]. Clinical and preclinical studies have reported that mitochondrial dysfunction indeed plays an essential role in insulin resistance, lipid metabolism, and follicular development [14,15]. However, the driving factors of hyperandrogenic disorders and their possible links to energy metabolism are still poorly understood, making current treatment options scarce [6,16].

In the current study, the adrenal H295R cell model is used to investigate the effect of mitochondrial dysfunction on androgen production. We show that inhibition of mitochondrial complex I by rotenone (Rot) induces a rapid shift towards hyperandrogenic steroidogenesis. Furthermore, we have performed a comprehensive bioenergetic screening of metabolic and mitochondrial inhibitors, which demonstrated stimulated DHEA production upon inhibition of complex I, III or mitochondrial pyruvate carrier. Our metabolomic studies reveal a common pattern of truncated tricarboxylic acid cycle metabolism with an inverse correlation of citric acid and DHEA production upon hyperandrogenic inhibitors. Taken together, our study demonstrates that androgen biosynthesis is tightly coupled to a dysfunctional mitochondrial environment. Specific alterations reported here could be explored in the future to identify novel molecular targets for the treatment of androgen excess disorders.

2. Materials and methods

2.1. Cell culture and drug exposure

The human adrenocortical cell line NCI-H295R was maintained in Dulbecco's modified Eagle's/Ham's F-12 medium containing L-glutamine and 15 mM HEPES (Thermo Fisher Scientific) supplemented with 5 % NU-I serum (BD Biosciences, Catalog ♯ 355500), insulin/transferrin/selenium (0.1 %), and penicillin (100 U/mL) and streptomycin (100 μg/mL). Cells were incubated at 37°C with 5 % CO_2 and divided at approximately 80 % confluence in T175 flasks. All inhibitors were purchased from Sigma, dissolved in dimethyl sulfoxide (DMSO) and diluted 0.01 % in culture medium to the indicated concentrations, except for 2-deoxy-D-glucose (2DG, 25 mM) and sodium citrate (0.5 M), which were dissolved directly in culture medium.

2.2. Cell metabolic analysis

Cells were seeded in XFe96-well plates (7'500/well) and analyzed using the Seahorse XFe96 real-time cell metabolic analyzer (Agilent Technologies). Cellular oxygen consumption rate (OCR) and extracellular acidification rate (ECAR) were assessed in DMEM medium supplemented with 10 mM glucose, 2 mM glutamine, 2 mM pyruvate and 5 mM HEPES. After initial assessment of basal OCR and ECAR rates, specific inhibitors were added as indicated, followed by injection of oligomycin (1 μM) to determine the oxidative leak, and the combined injection of Rot/ antimycin A (1 μM/ 1 μM) to determine non-mitochondrial respiration. Each experiment was normalized to cell number by Hoechst staining (1 μg/mL). For the calculation of specific steady-states, OCR was corrected for non-mitochondrial oxygen consumption. ATP production rates were calculated using Agilent Wave software (Agilent Technologies).

2.3. Steroid profiling by LC-MS or DHEA ELISA assay

Cells were seeded in 12-well plates ($1*10^6$/well) and exposed to specific inhibitors as indicated above. Quantification of complete steroid profiles in the culture supernatant was performed by liquid chromatography coupled to high-resolution mass spectrometry as previously described [17]. For direct assessment of DHEA, cells were seeded in 96-well plates (50'000/well) and after exposure to specific inhibitors, the supernatant was assessed by a DHEA ELISA assay kit according to the manufacturer's instructions (Catalog ♯ DHA31-K01, Eagle Biosciences). Results from both assays were normalized to total amount of protein using the DC protein determination assay (BioRad).

2.4. Untargeted metabolomics and targeted quantification of TCA cycle metabolites

Cells were seeded in 12-well plates ($1*10^6$/well), treated as indicated, washed with ammonium carbonate (75 mM, pH 7.4), and snap frozen in liquid nitrogen. For untargeted metabolomics, snap frozen cells were extracted with 70 % ethanol and analyzed by untargeted flow injection analysis on an Agilent 6550 Q-TOF instrument as previously described [18]. Ions were putatively annotated based on accurate mass against the KEGG database with a tolerance of 0.001 Da. For quantification of TCA cycle metabolites including citrate and isocitrate, snap frozen cells were extracted with 50 % acetonitrile and analyzed using liquid chromatography tandem mass spectrometry on a Shimadzu Nexera X2 LCX30 coupled to AB Sciex 6500+ Qtrap instrument as previously described [19]. Data was acquired with Analyst (version 1.7) and processed with SCIEX OS (version 3.1). Results were normalized to total amount of protein using the DC protein determination assay (BioRad).

2.5. Lipidomics

Cells were seeded in 12-well plates ($1*10^6$/well), treated as indicated and pellets were harvested. Collected pellets were extracted using 50:50 (v/v) methanol/isopropanol for 1 h at −20°C. Untargeted lipidomics was performed by reversed-phase liquid chromatography coupled to high-resolution mass spectrometry on a Thermo Fisher Q-Exactive HF-X mass spectrometer as previously described [20]. Data processing was performed using Compound Discoverer 3.1 (Thermo). Lipids were annotated with MS2 information and class-specific internal standards used for quantification.

2.6. Statistical analysis

All results are represented as the mean +/- standard error of the mean of at least three independent experiments. GraphPad Prism software (version 9) was used to plot graphs and perform statistical analysis, except for PCA analysis and heat map graphs, which were analyzed and plotted using MetaboAnalyst software (version 6.0). Data were analyzed by 2-tailed Student's t-test, unless otherwise indicated, and p-values of <0.05 (*) or <0.01 (**) were considered significant.

3. Results

3.1. Inhibition of mitochondrial complex I stimulates cellular androgen content

To test whether inhibition of aerobic respiration affects cellular androgen levels, we treated H295R cells with the mitochondrial complex I inhibitor Rot and conducted cell metabolic analysis and profiled steroidogenesis. As expected, Rot exposure caused an immediate and dose-dependent inhibition of mitochondrial respiration with a subsequent increase in anaerobic metabolism leading to a profound adaptation in the bioenergetic profile and a shift of calculated ATP production rates from aerobic to glycolytic metabolism (Fig. 1A-C, Suppl. Fig. 1 A-D). Exposure time up to 24 h at 200 nM Rot did not induce cellular cytotoxicity and resulted only in a mild accumulation of mitochondrial superoxide (Suppl. Fig. 1E-I). Time-dependent analysis of steroidogenic profiles (Fig. 2 A-M) revealed a rapid increase in DHEA after 2 h exposure to Rot, which further accumulated after 6 and 24 h (Fig. 2K). Further androgens, such as DHEA-sulfate (DHEAS), androstenedione (Adione), and testosterone, were stimulated only after 24 h (Fig. 2J, L, M). Other intermediates, such as pregnenolone (Preg), progesterone (Prog), 17αOH-pregnenolone (17αOH-Preg) and 17αOH-progesterone, were also increased after exposure to Rot (Fig. 2B, C, F, G). However, no significant stimulation of corticosterone or cortisol levels was observed, indicating no specific effect on mineralocorticoid or glucocorticoid accumulation (Fig. 2E, I). Based on the ratios of individual steroids to corresponding precursors, we implied related enzymatic activities in a subsidiary analysis (Suppl. Table 1). After 2 h of Rot exposure, we found decreased metabolic ratios of HSD3B2 (Prog/Preg and Adione/DHEA) and a slightly stimulated CYP17A1+CYB5A ratio (DHEA/17αOHPreg), which were not persistent after 6 or 24 h. Consistent with increased testosterone levels at 24 h, we found an increased 17β-hydroxysteroid dehydrogenase (HSD17B) enzymatic metabolic ratio at 24 h Rot exposure (Suppl. Table 1). Taken together, these results indicate that inhibition of aerobic respiration by Rot causes a rapid and profound shift in steroidogenesis towards androgen excess.

3.2. Specific mitochondrial dysfunction environments induce cellular DHEA excess

Based on the rapid onset of DHEA excess, we hypothesized that acute post-transcriptional metabolic adaptation is a major driver of the observed phenotype and characterized the metabolic adaptation in more detail. Knowing that Rot causes broad metabolic adaptations, we wanted to analyze whether other mitochondrial or metabolic disruptors have a similar ability to induce acute hyperandrogenic states. We therefore screened DHEA secretion in parallel with bioenergetic analysis after 6 h drug exposure using compound concentrations with an optimal metabolic output, but without a relevant cell proliferative effect (Fig. 3A-C). Exposure to the mitochondrial complex III inhibitor antimycin A (AA) caused a profound shift from aerobic to glycolytic metabolism and simultaneously stimulated DHEA accumulation. In contrast, inhibition of mitochondrial complex V by oligomycin (Oligo) also shifted metabolism to glycolysis but decreased DHEA secretion. Dissipation of mitochondrial membrane potential by the uncoupler FCCP (carbonylcyanide-p-trifluoromethoxyphenylhydrazone) shifted metabolism to a stressed metabolic phenotype with stimulated aerobic and anerobic metabolism, but was unable to affect DHEA secretion. Competitive inhibition of glycolysis by 2DG shifted metabolism toward higher aerobic metabolism and did not affect DHEA secretion. Interestingly, direct inhibition of the mitochondrial pyruvate carrier (MPC) by UK5099 (UK), which imports pyruvate into the mitochondrial matrix and thus promotes the direct flow of glycolytic flux into the mitochondria, increased DHEA levels and shifted the metabolic profile towards a similar glycolytic state as Rot. Other metabolic perturbations, such as inhibition of mitochondrial fatty acid uptake by Etomoxir (Eto) or inhibition of mitochondrial glutamine uptake by BPTES (bis-2-(5-phenylacetamido-1,2,4-thiadiazol-2-yl) ethyl sulfide 3), did not affect DHEA levels. Taken together, the screening suggests that acute inhibition of CI, CIII, or MPC stimulates DHEA accumulation in adrenal H295R cells.

3.3. Metabolic markers of truncated TCA cycle are associated with hyperandrogenic mitochondrial dysfunction

Next, we addressed the question of whether the hyperandrogenic inhibitors Rot, AA and UK share common metabolic drivers and examined the adaptive effects on the cellular metabolome and lipidome after 6 h drug exposure. We additionally compared the generated profiles with the non-androgenic OXPHOS inhibitor Oligo to exclude general metabolic effects upon mitochondrial dysfunction. Principal component analysis (PCA) of the assessed untargeted metabolome revealed clustering of biological replicates with preferential grouping of the OXPHOS inhibitors Rot, AA and Oligo versus DMSO and UK, thus not separating hyperandrogenic conditions (Fig. 4A). Analysis of the most altered metabolite ions (log2FC >0.5, adj. p-value <0.01) identified decreased intracellular (iso)citrate as a common marker in all hyperandrogenic treatments (Fig. 4B, Suppl. Table 2), while no common stimulated metabolic markers could be identified. Next, we analyzed tricarboxylic

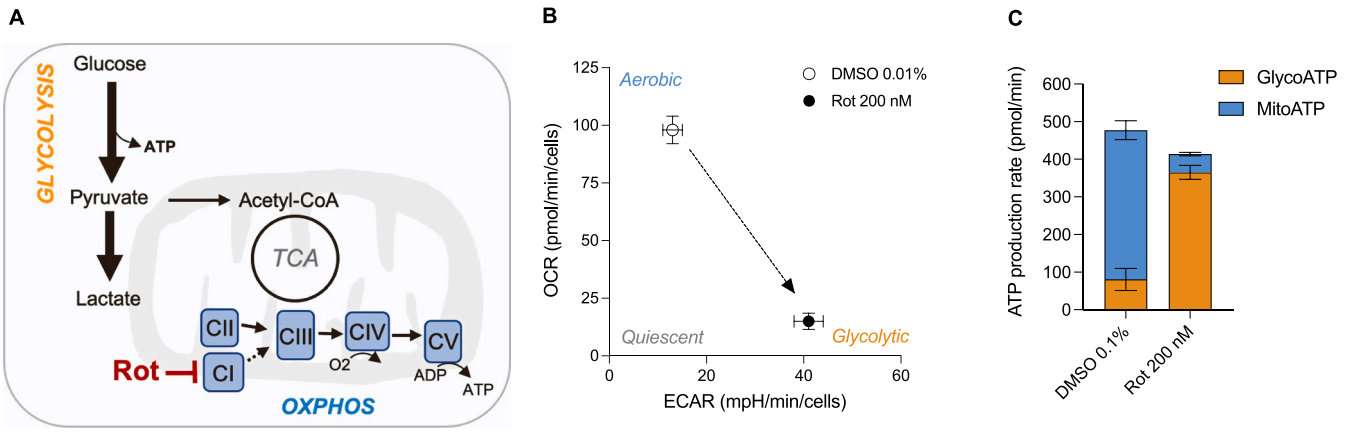

Fig. 1. Mitochondrial Complex I Inhibition shifts Metabolic Flux to Anaerobic Metabolism. A. Schematic representation of mitochondrial complex I inhibition by Rot, resulting in decreased oxidative phosphorylation (OXPHOS) and compensatory stimulation of glycolysis. Arrow thickness indicates stimulation or inhibition of the respective pathway. B. Bioenergetic plot showing shift towards anaerobic metabolism. Decreased oxygen consumption rate (OCR) and stimulated extracellular acidification rate (ECAR) were assessed by extracellular flux analysis after 6 h exposure to Rot (200 nM). C. Calculated ATP production rates from bioenergetic flux analysis.

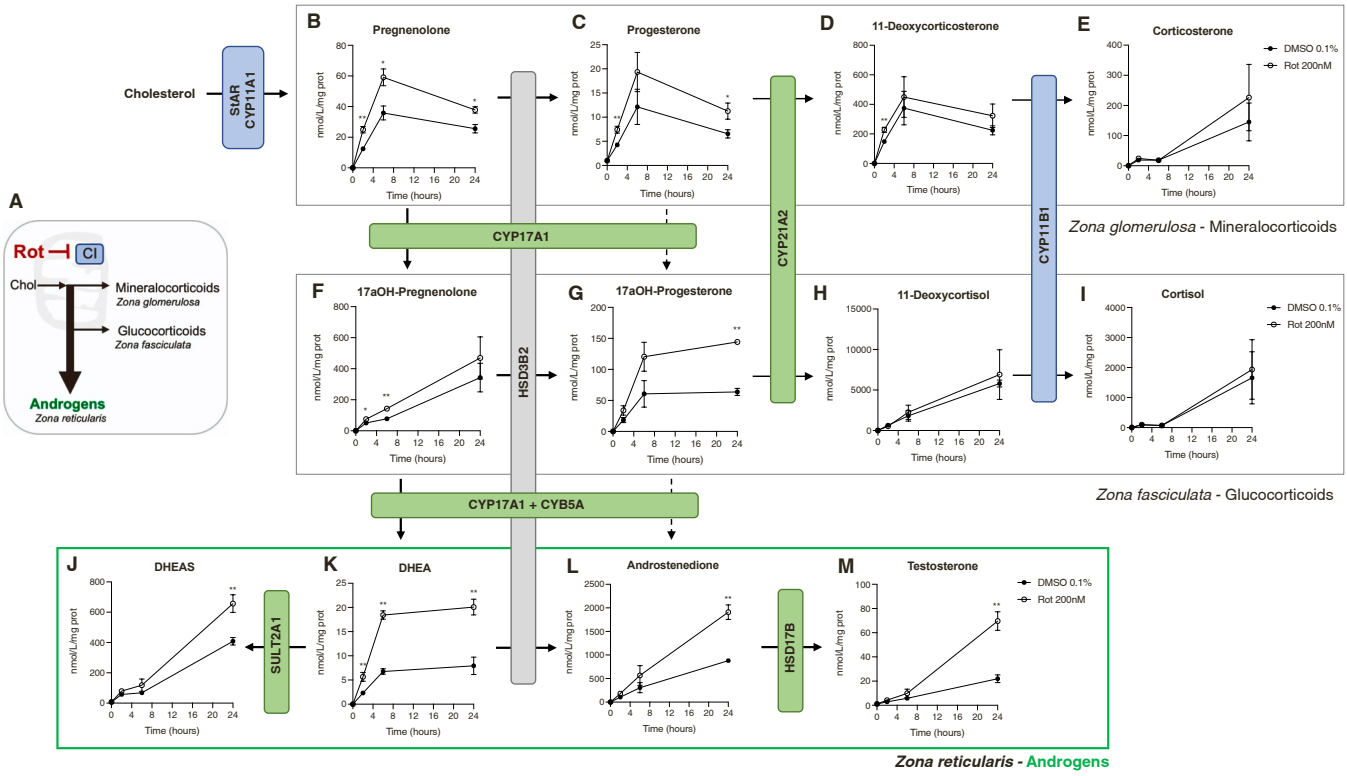

Fig. 2. Mitochondrial Complex I Inhibition drives Adrenal Steroidogenesis towards Androgen Biosynthesis. A. Schematic representation of steroidogenesis according to adrenal zonation, which is shifted toward androgen excess when inhibited at mitochondrial CI. B-M. Detailed assessment of steroidogenesis in H295R cells after exposure to 200 nM Rot for 0 h, 2 h, 6 h and 24 h. Steroidogenesis starts with mitochondrial cholesterol uptake and follows a cascade of specific enzymatic reactions. The time-dependent increase of the respective steroids in the cell culture supernatant was assessed using a mass spectrometry-based method. Each adrenal zonation profile is shown in the corresponding box; androgens are highlighted in green. The subcellular localization of each enzyme is color-coded as follows: mitochondrial (blue), ER (green), or mixed mitochondrial-ER (grey). Chol, Cholesterol; DHEA, dehydroepiandrosterone; DHEAS, dehydroepiandrosterone sulfate; StAR, steroid acute regulatory protein; CYP11A1, cytochrome P450 side chain cleavage; CYP21A2, cytochrome P450 21-hydroxylase; CYP11B1, cytochrome P450 aldosterone synthase; SULT2A1, sulfotransferase; HSD3B2, 3β-hydroxysteroid dehydrogenase; CYP17A1, cytochrome 17α-hydroxylase/17,20-lyase; CYB5, cytochrome b5; HSD17B, 17β-hydroxysteroid dehydrogenase.

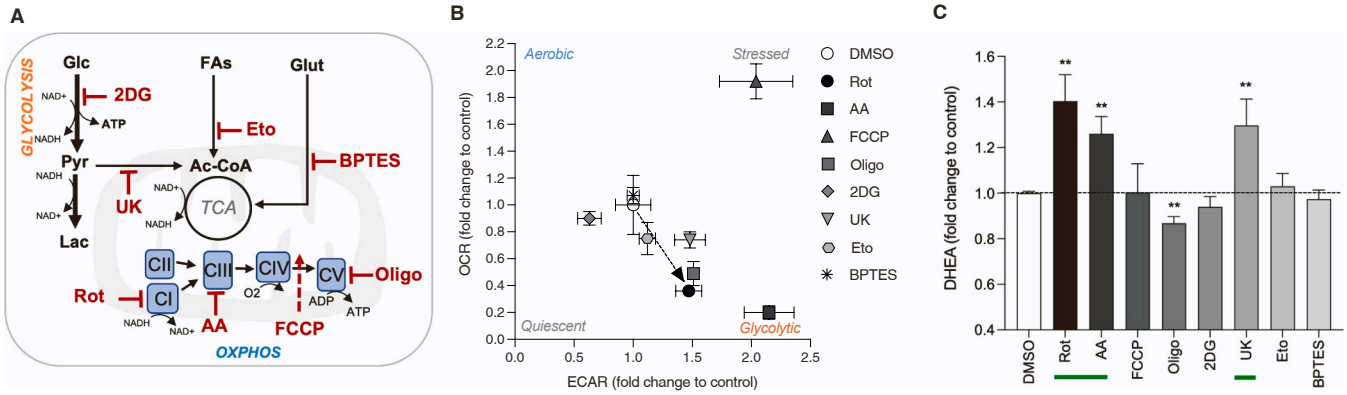

Fig. 3. Mitochondrial CI, CIII and MPC Inhibition stimulates DHEA Production. A. Schematic representation of the molecular targets of the various mitochondrial or metabolic inhibitors: OXPHOS inhibition at the level of Complex I with rotenone (Rot, 200 nM), Complex III with antimycin A (AA, 1 μM), Complex V with oligomycin (Oligo, 1 μM); uncoupling of mitochondrial electron transfer using the ionophore FCCP (carbonyl cyanide-p-trifluoromethoxyphenylhydrazone, 1 μM); competitive inhibition of glycolysis with 2-deoxy-D-glucose (2DG, 25 mM); inhibition of mitochondrial pyruvate uptake through mitochondrial pyruvate carrier (MPC) inhibitor UK5099 (UK, 3 μM); inhibition of mitochondrial fatty acid uptake by the carnitine-palmitoyl transferase 1 inhibitor Etomoxir (Eto, 3 μM); inhibition of mitochondrial glutamine uptake by the mitochondrial glutaminase inhibitor BPTES (bis-2-(5-phenylacetamido-1,3,4-thiadiazol-2-yl) ethyl sulfide, 3 μM). B. Bioenergetic plot showing the shift towards anaerobic or aerobic metabolism assessed by extracellular flux analysis after acute exposure to the respective inhibitors. C. Accumulation of DHEA in the supernatant after 6 h exposure to the respective inhibitors assessed by ELISA detection assay. Hyperandrogenic inhibitors are highlighted with a green underline (Rot, AA, UK). Abbreviations: Glc, glucose; Pyr, pyruvate; Lac, lactate; Ac-CoA, acetyl-CoA; FAs, fatty acids; Glut, glutamine; TCA, tricarboxylic acid cycle; OXPHOS, oxidative phosphorylation.

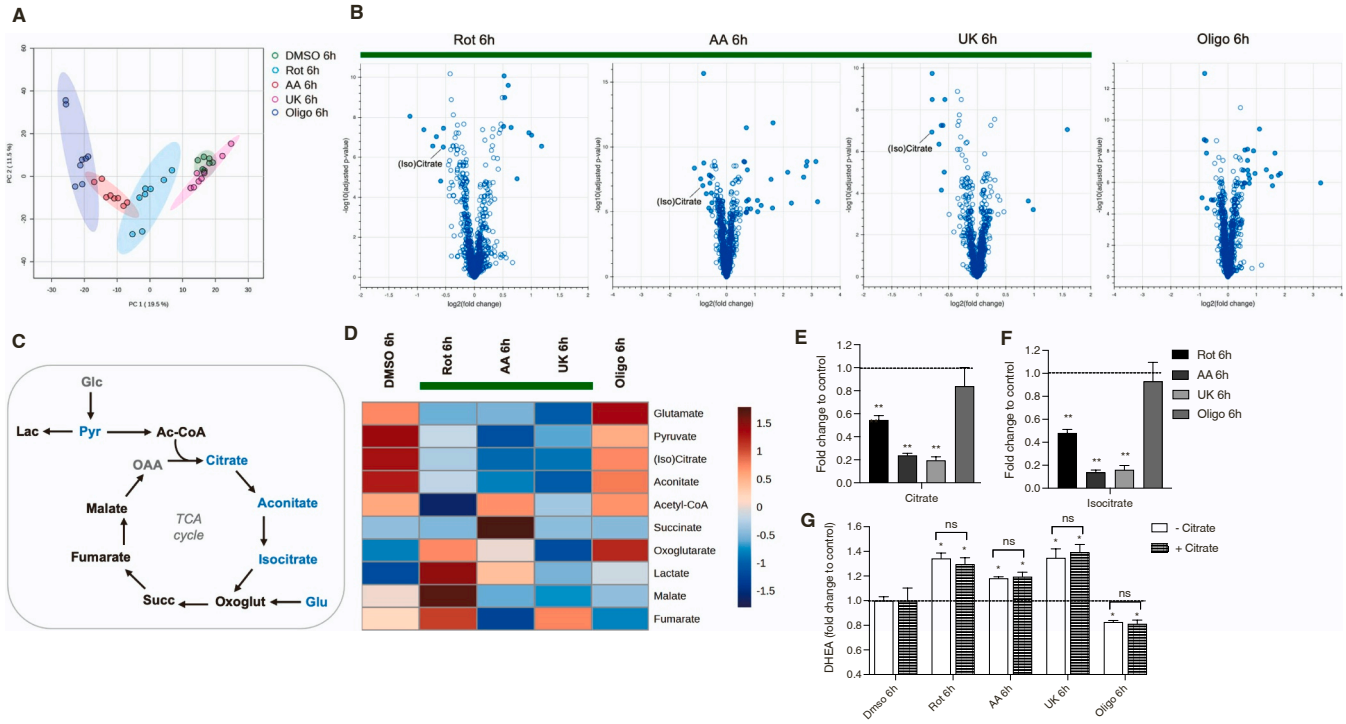

Fig. 4. Impaired TCA Cycle is Associated with Mitochondrial Dysfunction Causing DHEA Excess. A. Principal Component Analysis (PCA) with two principal components after 6 h of Rot, AA, UK, Oligo exposure versus DMSO control. B. Volcano plots showing statistically significant differences for the four treatments (closed blue dots log2FC >0.5, adj. p-value <0.01). Indicated is (iso)citrate as a common metabolite ion found in all hyperandrogenic treatments (highlighted with a green line). C-D. Schematic representation of TCA-associated metabolism and corresponding heatmap of detected metabolites using untargeted metabolomics. Hyperandrogenic treatments (highlighted with a green line) are characterized by decreased glutamate, pyruvate, (iso)citrate, and aconitate. E-F. Quantitative validation of intracellular citrate and isocitrate levels by targeted LC-MS analysis. G. Accumulation of DHEA in the supernatant after 6 h drug exposure with or without 0.5 mM citrate supplementation in the culture medium. DHEA levels were significantly changed compared to the respective control (*), while there was no significant (ns) change with additional citrate supplementation.

acid (TCA) cycle-related metabolite ions in more detail and additionally found that aconitate, pyruvate, and glutamate were decreased by all androgenic inhibitors (Fig. 4C-D). Targeted metabolite analysis confirmed decreased intracellular citrate and isocitrate levels in all hyperandrogenic treatments (Rot, AA, and UK), which was unaffected by the non-androgenic inhibitor Oligo (Fig. 4E-F). Finally, we tested the effect of direct supplementation of the cell culture medium with citrate, which did not affect DHEA levels after 6 h of drug exposure (Fig. 4G).

Knowing that hyperandrogenic states are associated with alterations in lipid metabolism [21,22], we additionally performed a lipidomic investigation to search for specific lipid markers. PCA again revealed a grouping of the OXPHOS inhibitors Rot, AA and Oligo versus DMSO and UK, thus not separating hyperandrogenic conditions (Fig. 5A). Analysis by total lipid class showed triglyceride accumulation in all OXPHOS inhibitors (Rot, AA, and Oligo) (Fig. 5B). Analysis of top altered lipid ions (log2FC >0.5, adj. p-value <0.01) did not identify a common hyperandrogenic marker, but additionally revealed an accumulation of unsaturated triglycerides upon exposure to OXPHOS inhibitors (Fig. 5C, Suppl. Table 3). Assuming that these lipids may be stored in intracellular lipid droplets, we performed additional studies using confocal imaging, but did not find any relevant reorganization of intracellular lipid droplet formation upon 24 h Rot exposure (Suppl. Fig. 2A-B). Taken together, these results demonstrate that the acute adaptive effect on the lipid desaturation response is associated with mitochondrial OXPHOS dysfunction induced by Rot, AA, and Oligo, whereas the common metabolic pattern upon hyperandrogenic condition induced by Rot, AA, and UK represents a dysfunctional TCA cycle.

4. Discussion

In this study, we describe a close interaction between mitochondrial bioenergetics and androgen biosynthesis in a steroid cell model. Our study shows that mitochondrial CI, CIII or MPC inhibition leads to a rapid DHEA accumulation. The three identified hyperandrogenic mitochondrial inhibitors have different molecular mechanisms: Rot affects mitochondrial NADH oxidation by inhibiting the transfer of electrons from CI to ubiquinone and thus still allowing convergent electron flow toward ubiquinone (e.g. through CII or alternative dehydrogenases). In contrast, AA inhibits the electron transfer of CIII from ubiquinol to cytochrome c, which effectively inhibits electron flow through the OXPHOS system [23]. Finally, inhibition of MPC by UK reduces the mitochondrial pyruvate uptake as a substrate for the TCA cycle and indirectly affects the respiratory capacity from pyruvate oxidation, thus stimulating the entry of alternative metabolites into the TCA cycle (e.g. through glutamine anaplerosis) [24].

We showed that the increase in DHEA is associated with a shift in cellular metabolism from aerobic to anaerobic glycolysis with a concomitant dysfunctional TCA cycle leading to decreased cellular citrate. Stimulation of anaerobic glycolysis has been described in patients with PCOS, with a strong positive correlation between lactate levels and insulin resistance [25]. Our study indicates that stimulated anaerobic glycolysis alone is not specific for hyperandrogenic condition, as shown by metabolic screening of various metabolic or mitochondrial inhibitors. In agreement with our *in vitro* study, metabolomic analysis performed in plasma of women with PCOS reported an inhibited TCA cycle with reduced citrate levels [25,26], suggesting similar systemic changes in whole-body metabolism. Citrate plays several important roles in cellular energy production and biosynthetic processes: It is a key intermediate in

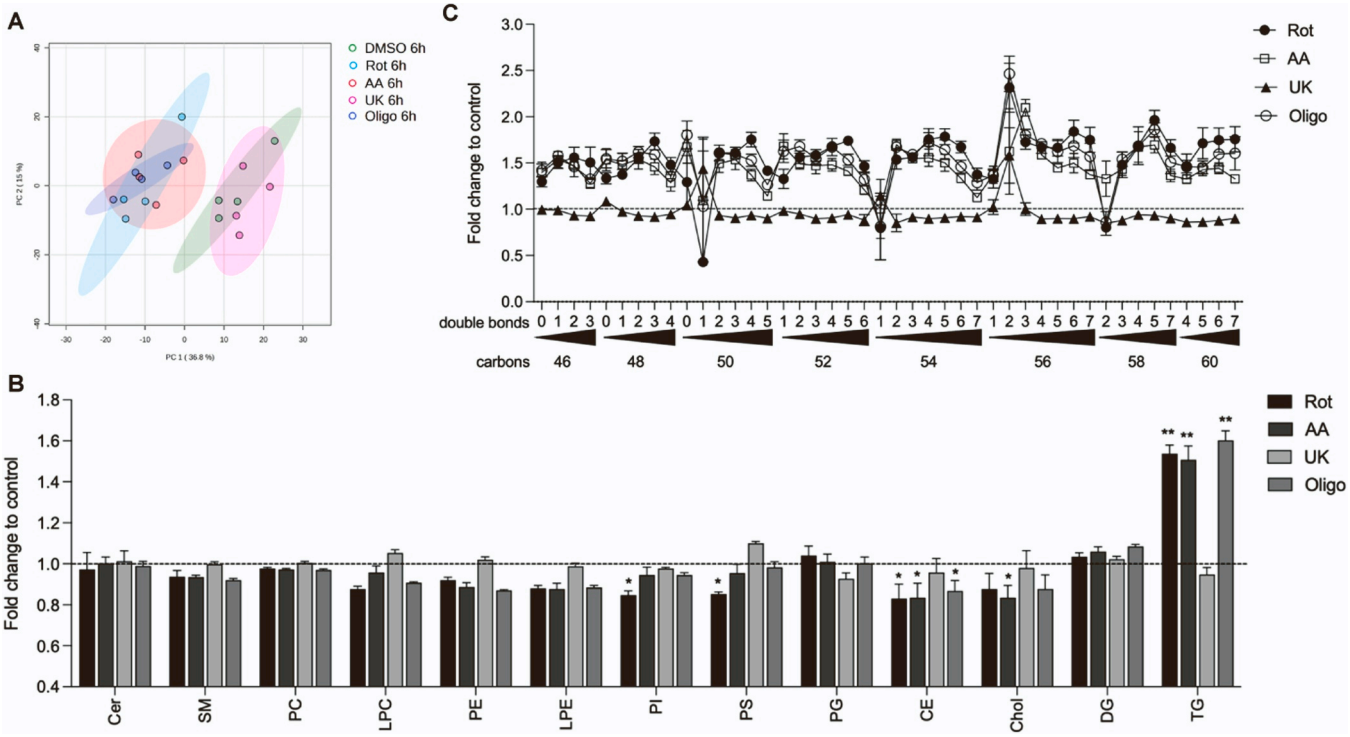

Fig. 5. TG Accumulation with Increased Desaturation Response is associated with OXPHOS Inhibition but not directly with DHEA Excess. A. Principal Component Analysis (PCA) with two principal components after 6 h of Rot, AA, UK, Oligo exposure versus DMSO control. B. Analysis by total lipid class. Statistical analysis was performed using 2-way ANOVA followed by Dunnett's multiple comparison test. C. Effect on cellular TGs differentiated along the x-axis based on total acyl chain carbon and double bond content. Top altered metabolites (log2FC >0.5, adj. p-value <0.01) are listed in Suppl. Table 3. Abbreviations: Cer, ceramides; SM, sphingomyelins; PC, phosphatidylcholines; LPC, lysophosphatidylcholines; PE, phosphatidylethanolamines; LPE, lysophosphatidylethanolamine; PI, phosphoinositides; PS, phosphatidylserine; PG, phosphatidylglycerols; CE, cholesterol esters; Chol, cholesterol; DG, diacylglycerols; TG, triglycerides.

the mitochondrial TCA cycle, where citrate synthase catalyzes the condensation of acetyl-CoA and oxaloacetate as a first step, and citrate is then further oxidized to produce reduction equivalents (NADH and $FADH_2$) for mitochondrial OXPHOS. It can also be transported to the cytoplasm via the mitochondrial citrate transporter, where ATP-citrate lyase generates acetyl-CoA for metabolic processes such as lipid biosynthesis. It is also a known inhibitor of phosphofructokinase and thus plays a regulatory role in glycolysis [27]. Consequently, low levels of citrate in the cytoplasm can stimulate glycolysis and are key features of the Warburg effect in tumor cells [28]. Since mitochondrial citrate production is the primary source for most cells, exogenous citrate transport is usually not of functional importance. Interestingly, RNA sequencing of microdissections of the human ZR identified SLC13A5, a plasma membrane sodium/citrate-cotransporter, as a highly expressed transporter [29,30]. This is a surprising finding that may indicate a nutrient-limited state in human ZR that has not been addressed so far. In our study, direct supplementation of citrate in the culture medium did not affect DHEA levels after hyperandrogenic treatment, suggesting that citrate itself may not be the main player, but rather a marker of an underlying metabolic adaptation leading to hyperandrogenic steroidogenesis.

Another hallmark of human hyperandrogenic conditions is an altered lipid status [21,22]. Our study found a decrease in cholesterolesters (CE) and an accumulation of total triglycerides (TGs) with a concomitant desaturation response to CI, CIII and CV inhibition, which was thus specific to OXPHOS inhibition but not to DHEA excess. The decreased cellular CE were concomitant with lower cholesterol levels, which might represent the previously described coregulation of mitochondrial function and cholesterol biosynthesis [31,32]. While the increased total TG may be the consequence of decreased energy-dependent mitochondrial fatty acid oxidation [33,34], the observed lipid desaturation response is related to stimulated ER metabolism, known as a mechanism for glycolytic NAD+ recycling [35] and highlights the close adaptive interplay between mitochondria and ER during mitochondrial dysfunction. Indeed, a detailed analysis of the ER-mitochondrial interplay may be important to gain further insight into the role of mitochondrial metabolism in the regulation of androgen synthesis. Steroidogenesis is performed in compartmentalized fashion between mitochondrial and ER subcellular compartments and is dependent on different subcellular redox pools and pairs, e.g. NADP(H) and NAD(H). ER-localized CYP17A1 is NADPH-dependent, which can be generated by anabolic reactions such as the cytosolic pentose phosphate pathway. HSD3B2, localized in the mitochondrial matrix but also in extramitochondrial compartments [36,37], depends on NAD+ and is therefore mainly associated with catabolic reactions. The relative lack of HSD3B2 expression/activity required for androgen production could thus be influenced by the pathways regulating mitochondrial NADH production and/or regulation of the subcellular distribution of HSD3B2.

The identification of several mitochondrial disruptors with hyperandrogenic effects supports the hypothesis that androgen excess is influenced by specific environments of mitochondrial dysfunction. Of course, the drugs reviewed in this study do not represent a complete survey of disruptors of mitochondrial metabolism. Therefore, it is highly likely that additional hyperandrogenic stimulators will be identified in subsequent studies. Several low-molecular weight drugs with off-target mitochondrial dysfunction have reached the market. One example is the anticonvulsant valproic acid, which has hyperandrogenic side effects [38,39] and is a well-known mitochondrial toxicant with diverse pathomechanisms on fatty acid oxidation and TCA cycle dysfunction [40]. Metformin is an insulin-sensitizing drug used as a treatment option for PCOS with a mechanism of action that is not fully understood [6,41]. It has been associated with CI inhibition *in vitro*, but this finding is related to supraphysiologic concentrations (1 mM) [42], which are not reached in humans and therefore do not contradict our results. Interestingly,

metformin is not an effective treatment option for all PCOS patients, suggesting that hyperandrogenic clinical phenotypes may be associated with multiple pathomechanisms.

The direct role of androgens and the androgen receptor (AR) in the regulation of glucose and lipid metabolism is well established. There is increasing evidence for a direct link between androgens and AR in the control of mitochondrial function [43,44]. For example, AR has been shown to be imported into and localized to mitochondria, where it has an inverse relationship with mitochondrial DNA content and thus negatively affects OXPHOS [45,46]. Furthermore, in prostate cancer cells, AR directly regulates the transcription of MPC2, a co-stabilizing protein of MPC, thus maintaining metabolic homeostasis by controlling the import of pyruvate into the mitochondrial matrix [47]. Taken together, these results provide further evidence to support the hypothesis of mitochondrial dysfunction associated with androgen excess.

Our study is limited in several ways. We used the H295R adrenal cancer cell line, which is a simplified system compared to a human, but is well established to study human steroidogenesis and is known to respond with a hyperandrogenic steroid profile under different cell culture conditions [48,49]. Consistent with our results, we have discussed confirmatory *in vitro* and *in vivo* data in the literature, so we are confident in the validity of our findings. To date, we have measured total levels of steroids and have not performed precursor labelled experiments to support where and how steroidogenesis is affected and whether other compensatory mechanisms occur. We also measured the total intracellular metabolomic content and have not provided a comprehensive picture of subcellular metabolites. Further resolution of metabolic adaptation is needed to specify differences in metabolic flux, e.g. through ^{13}C tracing and subcellular metabolite measurements. We have shown that different inhibitors of mitochondrial metabolism are fast drivers of DHEA production within 2–6 h, thus making strict genomic regulation unlikely, but gene expression profiling could add information to a potentially complex metabolic interplay.

In conclusion, our functional and metabolomic screening of mitochondrial dysfunction in adrenal H295R cells allowed us to identify a critical role for mitochondrial metabolism in androgen biosynthesis. The current data provide a starting point for further research to explore key metabolic drivers to provide specific pathomechanisms, identify predictive biomarkers, and advance the development of specific treatment options for patients with hyperandrogenic symptoms.

Funding

This work was funded by the KinderInsel grant (University Childrens Hospital Bern), which A.F. received. Metabolomics was supported by the ETH domain strategic focus area 'Personalized Health and Related Technology'.

CRediT authorship contribution statement

Déborah Mathis: Writing – review & editing, Methodology, Investigation, Formal analysis, Data curation. **Therina du Toit:** Writing – review & editing, Methodology, Investigation, Formal analysis, Data curation. **Emre Murat Altinkilic:** Writing – review & editing, Investigation. **Darko Stojkov:** Writing – review & editing, Investigation. **Christian Urzì:** Writing – review & editing, Investigation, Data curation. **Clarissa D. Voegel:** Writing – review & editing, Investigation, Data curation. **Vincen Wu:** Writing – review & editing, Formal analysis, Data curation. **Nicola Zamboni:** Writing – review & editing, Formal analysis, Data curation. **Hans-Uwe Simon:** Writing – review & editing, Methodology. **Jean-Marc Nuoffer:** Writing – review & editing, Methodology, Conceptualization. **Christa E. Flück:** Writing – review & editing, Methodology, Conceptualization. **Andrea Felser:** Writing – review & editing, Writing – original draft, Supervision, Project administration, Methodology, Investigation, Funding acquisition, Formal analysis, Data curation, Conceptualization.

Declaration of Competing Interest

The authors have declared no conflicts of interest.

Data Availability

Data will be made available on request.

Acknowledgements

We would like to thank the Research Committee of the University Children's Hospital Bern and especially Prof. Matthias Kopp for granting A.F. protected research time during her clinical training. Thanks also to Dr. Emanuele Pignatti for helpful discussions und suggestions, and Stefan Studer and Kay-Sara Sauter for administrative support. Images were acquired on equipment supported by the Microscopy Imaging Centre of the University of Bern.

Appendix A. Supporting information

Supplementary data associated with this article can be found in the online version at doi:10.1016/j.jsbmb.2024.106561.

References

[1] R. Naamneh Elzenaty, T. du Toit, C.E. Fluck, Basics of androgen synthesis and action, Best. Pr. Res Clin. Endocrinol. Metab. (2022) 101665.
[2] S.M. Black, J.A. Harikrishna, G.D. Szklarz, W.L. Miller, The mitochondrial environment is required for activity of the cholesterol side-chain cleavage enzyme, cytochrome P450scc, Proc. Natl. Acad. Sci. USA 91 (1994) 7247–7251.
[3] V. Papadopoulos, W.L. Miller, Role of mitochondria in steroidogenesis, Best. Pr. Res Clin. Endocrinol. Metab. 26 (2012) 771–790.
[4] W.L. Miller, Steroidogenesis: unanswered questions, Trends Endocrinol. Metab. 28 (2017) 771–793.
[5] P. Kempna, N. Marti, S. Udhane, C.E. Fluck, Regulation of androgen biosynthesis - a short review and preliminary results from the hyperandrogenic starvation NCI-H295R cell model, Mol. Cell Endocrinol. 408 (2015) 124–132.
[6] M.A. Sanchez-Garrido, M. Tena-Sempere, Metabolic dysfunction in polycystic ovary syndrome: Pathogenic role of androgen excess and potential therapeutic strategies, Mol. Metab. 35 (2020) 100937.
[7] E. Kousta, Premature adrenarche leads to polycystic ovary syndrome? Long-term consequences, Ann. N. Y. Acad. Sci. 1092 (2006) 148–157.
[8] W.L. Miller, Androgen synthesis in adrenarche, Rev. Endocr. Metab. Disord. 10 (2009) 3–17.
[9] T. Suzuki, H. Sasano, J. Takeyama, C. Kaneko, W.A. Freije, B.R. Carr, W.E. Rainey, Developmental changes in steroidogenic enzymes in human postnatal adrenal cortex: immunohistochemical studies, Clin. Endocrinol. (Oxf.) 53 (2000) 739–747.
[10] P. Shukla, S. Mukherjee, A. Patil, B. Joshi, Molecular characterization of variants in mitochondrial DNA encoded genes using next generation sequencing analysis and mitochondrial dysfunction in women with PCOS, Gene 855 (2023) 147126.
[11] P. Shukla, S. Mukherjee, Mitochondrial dysfunction: an emerging link in the pathophysiology of polycystic ovary syndrome, Mitochondrion 52 (2020) 24–39.
[12] X. Zeng, Q. Huang, S.L. Long, Q. Zhong, Z. Mo, Mitochondrial dysfunction in polycystic ovary syndrome, DNA Cell Biol. 39 (2020) 1401–1409.
[13] S.A. Dabravolski, N.G. Nikiforov, A.H. Eid, L.V. Nedosugova, A.V. Starodubova, T. V. Popkova, E.E. Bezsonov, A.N. Orekhov, Mitochondrial dysfunction and chronic inflammation in polycystic ovary syndrome, Int. J. Mol. Sci. 22 (2021).
[14] M. Das, C. Sauceda, N.J.G. Webster, Mitochondrial dysfunction in obesity and reproduction, Endocrinology 162 (2021).
[15] D. Sergi, N. Naumovski, L.K. Heilbronn, M. Abeywardena, N. O'Callaghan, L. Lionetti, N. Luscombe-Marsh, Mitochondrial (dys)function and insulin resistance: from pathophysiological molecular mechanisms to the impact of diet, Front Physiol. 10 (2019) 532.
[16] E. Diamanti-Kandarakis, A. Dunaif, Insulin resistance and the polycystic ovary syndrome revisited: an update on mechanisms and implications, Endocr. Rev. 33 (2012) 981–1030.
[17] T. Andrieu, T. du Toit, B. Vogt, M.D. Mueller, M. Groessl, Parallel targeted and non-targeted quantitative analysis of steroids in human serum and peritoneal fluid by liquid chromatography high-resolution mass spectrometry, Anal. Bioanal. Chem. 414 (2022) 7461–7472.
[18] T. Fuhrer, D. Heer, B. Begemann, N. Zamboni, High-throughput, accurate mass metabolome profiling of cellular extracts by flow injection-time-of-flight mass spectrometry, Anal. Chem. 83 (2011) 7074–7080.
[19] R. Rathod, B. Gajera, K. Nazir, J. Wallenius, V. Velagapudi, Simultaneous measurement of tricarboxylic acid cycle intermediates in different biological matrices using liquid chromatography-tandem mass spectrometry; quantitation and comparison of TCA cycle intermediates in human serum, plasma, kasumi-1 cell and murine liver tissue, Metabolites 10 (2020).

[20] S. Cherkaoui, S. Durot, J. Bradley, S. Critchlow, S. Dubuis, M.M. Masiero, R. Wegmann, B. Snijder, A. Othman, C. Bendtsen, N. Zamboni, A functional analysis of 180 cancer cell lines reveals conserved intrinsic metabolic programs, Mol. Syst. Biol. 18 (2022) e11033.
[21] A. Rajska, M. Buszewska-Forajta, D. Rachon, M.J. Markuszewski, Metabolomic insight into polycystic ovary syndrome-an overview, Int J. Mol. Sci. 21 (2020).
[22] A. Mousa, K. Huynh, S.J. Ellery, B.J. Strauss, A.E. Joham, B. de Courten, P. J. Meikle, H.J. Teede, Novel lipidomic signature associated with metabolic risk in women with and without polycystic ovary syndrome, J. Clin. Endocrinol. Metab. 107 (2022) e1987–e1999.
[23] D. Pesta, E. Gnaiger, High-resolution respirometry: OXPHOS protocols for human cells and permeabilized fibers from small biopsies of human muscle, Methods Mol. Biol. 810 (2012) 25–58.
[24] C. Yang, B. Ko, C.T. Hensley, L. Jiang, A.T. Wasti, J. Kim, J. Sudderth, M. A. Calvaruso, L. Lumata, M. Mitsche, J. Rutter, M.E. Merritt, R.J. DeBerardinis, Glutamine oxidation maintains the TCA cycle and cell survival during impaired mitochondrial pyruvate transport, Mol. Cell 56 (2014) 414–424.
[25] Y. Zhao, L. Fu, R. Li, L.N. Wang, Y. Yang, N.N. Liu, C.M. Zhang, Y. Wang, P. Liu, B. B. Tu, X. Zhang, J. Qiao, Metabolic profiles characterizing different phenotypes of polycystic ovary syndrome: plasma metabolomics analysis, BMC Med 10 (2012) 153.
[26] L. Sun, W. Hu, Q. Liu, Q. Hao, B. Sun, Q. Zhang, S. Mao, J. Qiao, X. Yan, Metabonomics reveals plasma metabolic changes and inflammatory marker in polycystic ovary syndrome patients, J. Proteome Res 11 (2012) 2937–2946.
[27] R.B. Crochet, J.D. Kim, H. Lee, Y.S. Yim, S.G. Kim, D. Neau, Y.H. Lee, Crystal structure of heart 6-phosphofructo-2-kinase/fructose-2,6-bisphosphatase (PFKFB2) and the inhibitory influence of citrate on substrate binding, Proteins 85 (2017) 117–124.
[28] P. Icard, A. Coquerel, Z. Wu, J. Gligorov, D. Fuks, L. Fournel, H. Lincet, L. Simula, Understanding the Central Role of Citrate in the Metabolism of Cancer Cells and Tumors: An Update, Int J. Mol. Sci. 22 (2021).
[29] J. Rege, Y. Nakamura, T. Wang, T.D. Merchen, H. Sasano, W.E. Rainey, Transcriptome profiling reveals differentially expressed transcripts between the human adrenal zona fasciculata and zona reticularis, J. Clin. Endocrinol. Metab. 99 (2014) E518–E527.
[30] J.E. Baker, S.W. Plaska, Z. Qin, C.J. Liu, J. Rege, W.E. Rainey, A.M. Udager, Targeted RNA sequencing of adrenal zones using immunohistochemistry-guided capture of formalin-fixed paraffin-embedded tissue, Mol. Cell Endocrinol. 530 (2021) 111296.
[31] C.T.J. Wall, G. Lefebvre, S. Metairon, P. Descombes, A. Wiederkehr, J. Santo-Domingo, Mitochondrial respiratory chain dysfunction alters ER sterol sensing and mevalonate pathway activity, J. Biol. Chem. 298 (2022) 101652.
[32] I. Kuhl, M. Miranda, I. Atanassov, I. Kuznetsova, Y. Hinze, A. Mourier, A. Filipovska, N.G. Larsson, Transcriptomic and proteomic landscape of mitochondrial dysfunction reveals secondary coenzyme Q deficiency in mammals, Elife 6 (2017).
[33] Q. He, M. Wang, C. Petucci, S.J. Gardell, X. Han, Rotenone induces reductive stress and triacylglycerol deposition in C2C12 cells, Int J. Biochem Cell Biol. 45 (2013) 2749–2755.
[34] S. Vankoningsloo, M. Piens, C. Lecocq, A. Gilson, A. De Pauw, P. Renard, C. Demazy, A. Houbion, M. Raes, T. Arnould, Mitochondrial dysfunction induces triglyceride accumulation in 3T3-L1 cells: role of fatty acid beta-oxidation and glucose, J. Lipid Res 46 (2005) 1133–1149.
[35] W. Kim, A. Deik, C. Gonzalez, M.E. Gonzalez, F. Fu, M. Ferrari, C.L. Churchhouse, J.C. Florez, S.B.R. Jacobs, C.B. Clish, E.P. Rhee, Polyunsaturated fatty acid desaturation is a mechanism for glycolytic NAD(+) recycling, Cell Metab. 29 (2019) 856–870, e857.
[36] N. Cherradi, E.M. Chambaz, G. Defaye, Organization of 3 beta-hydroxysteroid dehydrogenase/isomerase and cytochrome P450scc into a catalytically active molecular complex in bovine adrenocortical mitochondria, J. Steroid Biochem. Mol. Biol. 55 (1995) 507–514.
[37] J. Yu, L. Zhang, Y. Li, X. Zhu, S. Xu, X.M. Zhou, H. Wang, H. Zhang, B. Liang, P. Liu, The adrenal lipid droplet is a new site for steroid hormone metabolism, Proteomics 18 (2018) e1800136.
[38] A. Sharma, C.K. Welt, Practical Approach to Hyperandrogenism in Women, Med Clin. North Am. 105 (2021) 1099–1116.
[39] C.E. Fluck, D.C. Yaworsky, W.L. Miller, Effects of anticonvulsants on human p450c17 (17alpha-hydroxylase/17,20 lyase) and 3beta-hydroxysteroid dehydrogenase type 2, Epilepsia 46 (2005) 444–448.
[40] K. Begriche, J. Massart, M.A. Robin, A. Borgne-Sanchez, B. Fromenty, Drug-induced toxicity on mitochondria and lipid metabolism: mechanistic diversity and deleterious consequences for the liver, J. Hepatol. 54 (2011) 773–794.
[41] T.E. LaMoia, G.I. Shulman, Cellular and molecular mechanisms of metformin action, Endocr. Rev. 42 (2021) 77–96.
[42] A. Hirsch, D. Hahn, P. Kempna, G. Hofer, J.M. Nuoffer, P.E. Mullis, C.E. Fluck, Metformin inhibits human androgen production by regulating steroidogenic enzymes HSD3B2 and CYP17A1 and complex I activity of the respiratory chain, Endocrinology 153 (2012) 4354–4366.
[43] L. Yin, S. Qi, Z. Zhu, Advances in mitochondria-centered mechanism behind the roles of androgens and androgen receptor in the regulation of glucose and lipid metabolism, Front Endocrinol. (Lausanne) 14 (2023) 1267170.
[44] I. Ahmad, A.E. Newell-Fugate, Role of androgens and androgen receptor in control of mitochondrial function, Am. J. Physiol. Cell Physiol. 323 (2022) C835–C846.
[45] P. Bajpai, E. Koc, G. Sonpavde, R. Singh, K.K. Singh, Mitochondrial localization, import, and mitochondrial function of the androgen receptor, J. Biol. Chem. 294 (2019) 6621–6634.
[46] A. Lerner, D. Kewada, A. Ahmed, K. Hardy, M. Christian, S. Franks, Androgen reduces mitochondrial respiration in mouse brown adipocytes: a model for disordered energy balance in polycystic ovary syndrome, Int. J. Mol. Sci. 22 (2020).
[47] D.A. Bader, S.M. Hartig, V. Putluri, C. Foley, M.P. Hamilton, E.A. Smith, P.K. Saha, A. Panigrahi, C. Walker, L. Zong, H. Martini-Stoica, R. Chen, K. Rajapakshe, C. Coarfa, A. Sreekumar, N. Mitsiades, J.A. Bankson, M.M. Ittmann, B.W. O'Malley, N. Putluri, S.E. McGuire, Mitochondrial pyruvate import is a metabolic vulnerability in androgen receptor-driven prostate cancer, Nat. Metab. 1 (2019) 70–85.
[48] A.F. Gazdar, H.K. Oie, C.H. Shackleton, T.R. Chen, T.J. Triche, C.E. Myers, G. P. Chrousos, M.F. Brennan, C.A. Stein, R.V. La Rocca, Establishment and characterization of a human adrenocortical carcinoma cell line that expresses multiple pathways of steroid biosynthesis, Cancer Res. 50 (1990) 5488–5496.
[49] E. Pignatti, E.M. Altinkilic, K. Brautigam, M. Grossl, A. Perren, M. Zavolan, C. E. Fluck, Cholesterol deprivation drives DHEA biosynthesis in human adrenals, Endocrinology 163 (2022).